

# Molecular Recognition Properties of Acyclic Cucurbiturils Toward Amino Acids, Peptides, and a Protein

*Sandra A. Zebaze Ndendjio and Lyle Isaacs\**

Department of Chemistry and Biochemistry, University of Maryland, College Park, MD 20742,  
United States

\*To whom correspondence should be addressed. Prof. Lyle Isaacs, Department of Chemistry  
and Biochemistry, University of Maryland, College Park, MD 20742, USA. Phone 301-405-  
1884; Email: [LIsaacs@umd.edu](mailto:LIsaacs@umd.edu); Fax: 301-314-9121

---

**Abstract:** We report the binding of acyclic CB[n] **1** and **2** toward 19 amino acid amides by <sup>1</sup>H NMR and isothermal titration calorimetry. Hosts **1** and **2** bind the aromatic or hydrophobic residues by cavity inclusion leaving the cationic residues at the C=O portals.  $K_a$  values range from  $10^2$  to  $>10^6$  M<sup>-1</sup> with the aromatic amino acid amides H-Phe-NH<sub>2</sub>, H-Trp-NH<sub>2</sub>, and H-Tyr-NH<sub>2</sub> displaying sub-micromolar  $K_d$  values. Hosts **1** and **2** bind tightly to dicationic H-Lys-NH<sub>2</sub> and H-Arg-NH<sub>2</sub> which are poor guests for macrocyclic CB[7]. Comparison of the affinity of **1** and **2** toward the amino acid amide, N-acetyl-amino-acid amide, and amino acid forms of Phe revealed that the removal of the NH<sub>3</sub><sup>+</sup> to O=C and SO<sub>3</sub><sup>-</sup> electrostatic interactions costs 3.8 kcal/mol whereas the introduction of an unfavorable CO<sub>2</sub><sup>-</sup> to O=C and SO<sub>3</sub><sup>-</sup> electrostatic interactions costs 2.1 kcal/mol. Seven tripeptides (FXA; X=G,L,I,V,P,F,K) were investigated to explore the potential of double residue inclusion which, unfortunately, was not detected. Just like CB[7], **1** and **2** bind to insulin with low micromolar affinity. Acyclic CB[n] display a high affinity toward a wider range of N-terminal amino acids residues than macrocyclic CB[n] which suggests a broad range of applications of this class of hosts.

---

Keywords: acyclic cucurbituril, molecular recognition, amino acid, peptide, isothermal titration microcalorimetry

**Introduction.** The synthetic and supramolecular chemistry of the CB[n] family has played a leading role in the field since the preparation of cucurbit[n]uril homologues (CB[n], Figure 1) at the turn of the millennium.<sup>12</sup> CB[n] compounds are powerful receptors for hydrophobic (di)cations in aqueous solution due to their two symmetry equivalent ureidyl carbonyl lined portals which guard entry to a hydrophobic cavity.<sup>3</sup> For example, the  $K_a$  for CB[7]•guest complexes routinely exceed  $10^6$  M<sup>-1</sup>, often exceed  $10^9$  M<sup>-1</sup>, and in special cases (e.g. cationic adamantanes and diamantanes) can even exceed  $10^{12}$  M<sup>-1</sup> in water due to the combined effects of ion-dipole interactions and the hydrophobic effect.<sup>3-4</sup> In addition to high affinity binding, CB[n]•guest complexes also display high stimuli responsiveness (e.g. pH, electrochemistry, photochemistry, competing guest) which allows for the use of CB[n] in a variety of applications.<sup>2b,5</sup> For example, CB[7]•guest binary complexes and CB[8]•guest1•guest2 ternary complexes are used to construct molecular switches and machines,<sup>5c</sup> as supramolecular catalysts,<sup>2a,6</sup> to solubilize, protect, sequester, and even create targeted pharmaceuticals,<sup>7</sup> as components of chemical sensors,<sup>89</sup> and to promote the assembly of supramolecular polymers, materials, and frameworks.<sup>10</sup> CB[n] have also found wide applicability in peptide and protein chemistry. For example, in pioneering work, the Urbach group showed that CB[8] promotes the cooperative dimerization of the Phe-Gly-Gly peptide in water via formation of the CB[8]•(Phe-Gly-Gly)<sub>2</sub> complex with  $K_a = 1.5 \times 10^{11}$  M<sup>-2</sup>.<sup>11</sup> This motif has been capitalized upon by Brunsved and Liu to promote the dimerization of proteins tagged with N-terminal FGG units and thereby control biological functions.<sup>12</sup> For example, Brunsved engineered a split luciferase<sup>13</sup> that could be reconstituted by addition of CB[8] and similarly CB[8] was found to promote the dimerization of monomeric caspase-9 into the active dimer.<sup>14</sup> Scherman has used the FGG motif to promote hydrogel formation.<sup>15</sup> In a lovely series of papers, Urbach and

collaborators demonstrated that the N-terminus of peptides and proteins is a privileged site for host complexation due to simultaneous ammonium ion and side chain binding (Figure 2). In particular, they found that CB[7] displays a selectivity toward N-terminal Phe over other N-terminal residues presumably because they display suboptimal fit for the CB[7] cavity (e.g. other aromatic or hydrophobic amino acids may not fully release cavity waters of solvation) or because they cannot sterically accommodate N-terminus and cationic sidechain binding (e.g. Lys, His, Arg). The CB[7]•N-terminal Phe motif was used to recognize Insulin in solution and on resin, to determine protease substrate selectivity, to impose sequence specific inhibition on a nonspecific protease, and for supramolecular enhancement of protein analysis.<sup>16</sup> Recently, Langer, Anderson, and Isaacs used a monofunctionalized CB[7] derivative to non-covalently PEGylate the N-terminal Phe residue of Insulin and thereby prolong its *in vivo* function.<sup>17</sup>

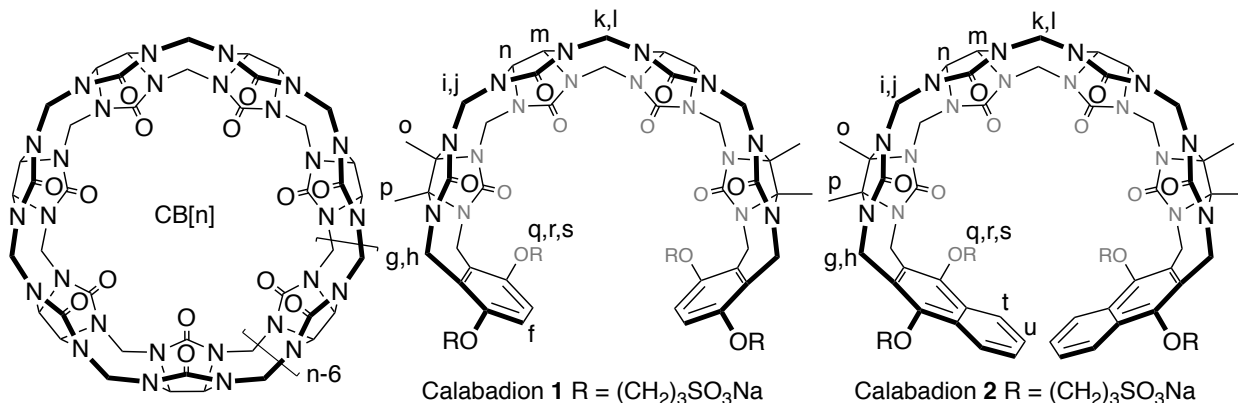


**Figure 1.** Chemical structures of CB[n] and Calabadions 1 and 2.

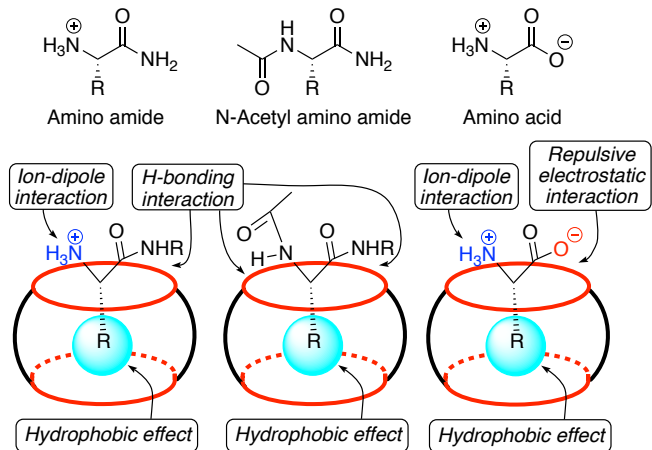


**Figure 2.** Chemical structure of amino acids, amino amides, and N-acetyl amino amides used as guests in this study and illustration of the geometries and driving forces involved in their complexation with macrocyclic CB[n].

In recent years, the Isaacs group has synthesized and investigated the molecular recognition properties of acyclic CB[n]-type receptors that feature a central glycoluril oligomer, two terminal aromatic walls, and four sulfonate solubilizing groups.<sup>2c</sup> Two prototypical acyclic CB[n] (Calabadion **1** and Calabadion **2**) are shown in Figure 1 although numerous variants are known.<sup>18</sup> The Calabadions retain the essential molecular recognition features of CB[n], but because they are acyclic they are able to flex their methylene bridged glycoluril oligomer backbone to accommodate more voluminous guests. Additionally, the acyclic structure of the Calabadions may allow guest substituents to protrude through the side of the host•guest complex rather than through the portals as required for macrocyclic CB[n]. The Calabadions have several important biomedical applications including the solubilization of insoluble anticancer drugs for *in vivo* application,<sup>18d,19</sup> as agents to reverse neuromuscular block *in vivo*,<sup>20</sup> and most recently to modulate the hyperlocomotor activity of rats treated with methamphetamine.<sup>21</sup> Recently the Ma group has been using acyclic CB[n] for acid sensitive controlled release and bioimaging

applications.<sup>22</sup> By virtue of their aromatic walls, Calabadions undergo changes in their UV/Vis and fluorescence properties upon guest binding and have therefore been used as sensors for nitrosamines, over-the-counter drugs, amino acids, and opioids.<sup>8b,23</sup> Given the ability of CB[7] and CB[8] to interact with peptide N-termini and internal residues, protein N-termini, and to promote dimerization and the fact that Calabadions retain the essential recognition properties of macrocyclic CB[n] we hypothesized that **1** and **2** would perform well in peptide and protein recognition perhaps with selectivity that is complementary to that observed for CB[n].

**Results and Discussion.** This results and discussion section is organized as follows. First, we lay out the goals and the hypotheses to be tested in this study. Next, we describe <sup>1</sup>H NMR investigations of the binding properties of **1** and **2** toward 19 amino acid amides to confirm the 1:1 binding stoichiometry and shed light on the geometrical features of the complexes. Next, we present the energetics ( $\Delta G$ ,  $\Delta H$ ,  $\Delta S$ ) of binding of **1** and **2** toward the various amino amides by isothermal titration calorimetry. Subsequently, we detail the influence of electrostatics on the energetics of host•guest binding as probed through mutation of amino acid to amino acid amide to N-acetyl amino acid amide. Next, we present the binding of **1** and **2** toward selected tripeptides to delineate the influence of neighboring residues. Finally, we present the results of binding of **1** and **2** toward insulin compared to CB[7].

**Goals of the Study.** Macroyclic CB[7] selectively recognizes peptides that feature an N-terminal hydrophobic aromatic residue like Phe or Trp due to a combination of ion-dipole interactions and the hydrophobic effect and discriminates against residues containing hydrophobic aliphatic side chains, polar neutral side chains, acidic (anionic) side chains, and

even basic (cationic) side chains.<sup>11b,16b,24</sup> The discrimination of CB[7] against the residues with cationic side chains (e.g. Lys and Arg) is due to the fact that the sidechain cannot thread through the cavity to form ion-dipole interactions at both portals without creating steric interactions between the wall of CB[7] and the adjacent CONHR group. We hypothesized that acyclic CB[n] **1** and **2** – with their acyclic structure – would display higher affinity toward Lys and Arg and because the steric constraints of these amino acids might be better accommodated.<sup>25</sup> Accordingly, a primary goal of the work is the measurement of the binding affinity of **1** and **2** toward the amino acid amides which mimics the context of the amino acid in a longer peptide. Within this realm, we also sought to compare the peptide recognition properties of **1** and **2** which differ in the nature of their aromatic walls, cavity size, and presumably their selectivity toward aromatic amino acids in particular. Given the ability of CB[8] to bind two residues simultaneously,<sup>11b,15a</sup> we were aware of the possibility of similar behavior with **2** (or **1**) and were careful to verify the binding stoichiometry. Given that **1** and **2** are tetra-anionic in pH 7.4 water whereas CB[7] is neutral at this pH we sought, as a secondary goal, to understand the role of electrostatics on the molecular recognition properties of **1** and **2** toward amino amides, N-acetyl amino amides, and amino acids themselves. Finally, we wanted to examine the recognition properties of **1** or **2** toward N-terminal amino acid in the context of a protein (insulin).

***<sup>1</sup>H NMR Investigations of Calabadion•Guest Binding.*** First, we investigated the binding interactions between **1** and **2** toward amino acid amides by <sup>1</sup>H NMR spectroscopy. We performed these experiments in biologically relevant 20 mM sodium phosphate buffered D<sub>2</sub>O at pD 7.4 to ensure that the N-terminus of each amino acid amide is present as its NH<sub>3</sub><sup>+</sup> form which provides a primary binding site for hosts **1** and **2**. As documented in the Supporting Information

for 19 amino acid amides (excluding cysteine), we measured  $^1\text{H}$  NMR spectra at different host:guest ratios (generally 1:2, 1:1.5, 1:1, and 1:0.5). We monitored the change in guest chemical shifts upon complexation to provide crude information on host•guest stoichiometry and to determine whether the kinetics of guest exchange is in the fast, intermediate, or slow exchange regime on the  $^1\text{H}$  NMR timescale. Rather than discuss the precise changes for each host•guest complex, we discuss here some general trends that are observed in the chemical shifts of both host and guest upon complexation. For example, Figure 3 shows the  $^1\text{H}$  NMR spectra recorded for mixtures of **1** and H-Phe-NH<sub>2</sub>. A comparison of Figure 3a and 3d shows that the protons on the aromatic ring of H-Phe-NH<sub>2</sub> (H<sub>c</sub> – H<sub>e</sub>) and the adjacent benzylic CH<sub>2</sub> group (H<sub>b</sub>) undergo a substantial upfield change in chemical shift upon complexation (H<sub>c</sub> – H<sub>e</sub>; 1 – 1.5 ppm; H<sub>b</sub>  $\approx$  0.8 ppm) which strongly suggests that the Ar-ring and benzylic CH<sub>2</sub> of H-Phe-NH<sub>2</sub> is bound within the cavity of **1** within the **1**•H-Phe-NH<sub>2</sub> complex. Conversely, the  $\alpha$ -proton H<sub>a</sub> of H-Phe-NH<sub>2</sub> undergoes a slight downfield shift ( $\approx$  0.2 ppm) upon complex formation which indicates that H<sub>a</sub> is located nearby the deshielding region defined by the ureidyl C=O groups of the host. When an excess of H-Phe-NH<sub>2</sub> is present (e.g. 1:2, Figure 3b) the resonances for H<sub>c</sub> – H<sub>e</sub> shift back toward the position observed for uncomplexed H-Phe-NH<sub>2</sub> and broaden which indicates that this complex displays intermediate exchange kinetics on the  $^1\text{H}$  NMR timescale and likely has 1:1 stoichiometry. In accord with this data and based on the known binding preferences of CB[n] and acyclic CB[n], we formulate the geometry of the **1**•H-Phe-NH<sub>2</sub> complex as illustrated in Figure 4a. We believe that the amide (C=O)NH<sub>2</sub> group of H-Phe-NH<sub>2</sub> is hydrogen bonded to the ureidyl C=O group of host **1** in the complex.<sup>11a</sup> Related changes are observed during the complexation of the hydrophobic amino acid amides (Supporting Information) indicating that side chain cavity inclusion and NH<sub>3</sub><sup>+</sup> portal binding is the dominant geometry. Changes are also

observed in the  $^1\text{H}$  NMR resonance for host **1** in the **1**•H-Phe-NH<sub>2</sub> complex. For example, the H<sub>f</sub> protons in  $C_{2v}$ -symmetric **1** are symmetry equivalent and display a sharp singlet (Figure 3f) but become broadened and split upon formation of the  $C_1$ -symmetric (e.g. no symmetry) **1**•H-Phe-NH<sub>2</sub> complex. This observation can be explained by the fact that the chiral host•guest complex renders all four H<sub>f</sub> atoms diastereotopic. In the case of fast kinetics of exchange, typified beautifully by the **1**•H-Leu-NH<sub>2</sub> complex, two doublets are observed for H<sub>f</sub> (Supporting Information, Figure S86). Related observations are observed with host **2**. None of the complexes between **1** or **2** and the amino acid amides displayed slow kinetics of exchange on the  $^1\text{H}$  NMR timescale. Interestingly, for complexes between **1** (**2**) and the hydrophobic non-aromatic amino acid amides, we typically observe a small downfield shift for host aromatic sidewall resonance H<sub>f</sub>, H<sub>t</sub>, H<sub>u</sub> (**1**: up to 0.3 ppm; **2**: up to 0.5 ppm). As described previously in related systems, we believe this is due to a conformational change that hosts **1** and **2** undergo upon complexation that removes edge-to-face C-H $\cdots\pi$  interactions that occur in the uncomplexed host that result in upfield shifting.<sup>2c</sup> In contrast, for the aromatic amino acid amides (e.g. H-Trp-NH<sub>2</sub>, H-Tyr-NH<sub>2</sub>, H-Phe-NH<sub>2</sub>) only very small changes in chemical shift are observed for H<sub>f</sub> which we believe reflects a balance between the expected downfield shift due to conformational change and upfield shift due to the shielding effect of the aromatic ring of the guest. Interestingly, we found no evidence by  $^1\text{H}$  NMR of binding of **1** or **2** (at mM concentrations) toward Asp and Glu which contain CO<sub>2</sub>H groups in their side chains that are expected to be present in their anionic CO<sub>2</sub><sup>-</sup> form at pD 7.4. This result is in accord with previous observations from CB[n] molecular recognition that the electrostatically negative ureidyl C=O portals do not tolerate the presence of guest negative charge at the portals.<sup>4b,4e</sup> Furthermore, the presence of the SO<sub>3</sub><sup>-</sup> solubilizing groups on **1** and **2** would be expected to

electrostatically destabilize complexes with Asp and Glu. Finally, for H-Gly-NH<sub>2</sub>, H-Ala-NH<sub>2</sub>, and H-Ser-NH<sub>2</sub> which have no, small, or hydrophilic side chains we observe only small changes (e.g.  $\Delta\delta$  and broadening) in the <sup>1</sup>H NMR which probably indicates very weak binding or non-inclusion binding (e.g. portal binding) or a combination thereof.

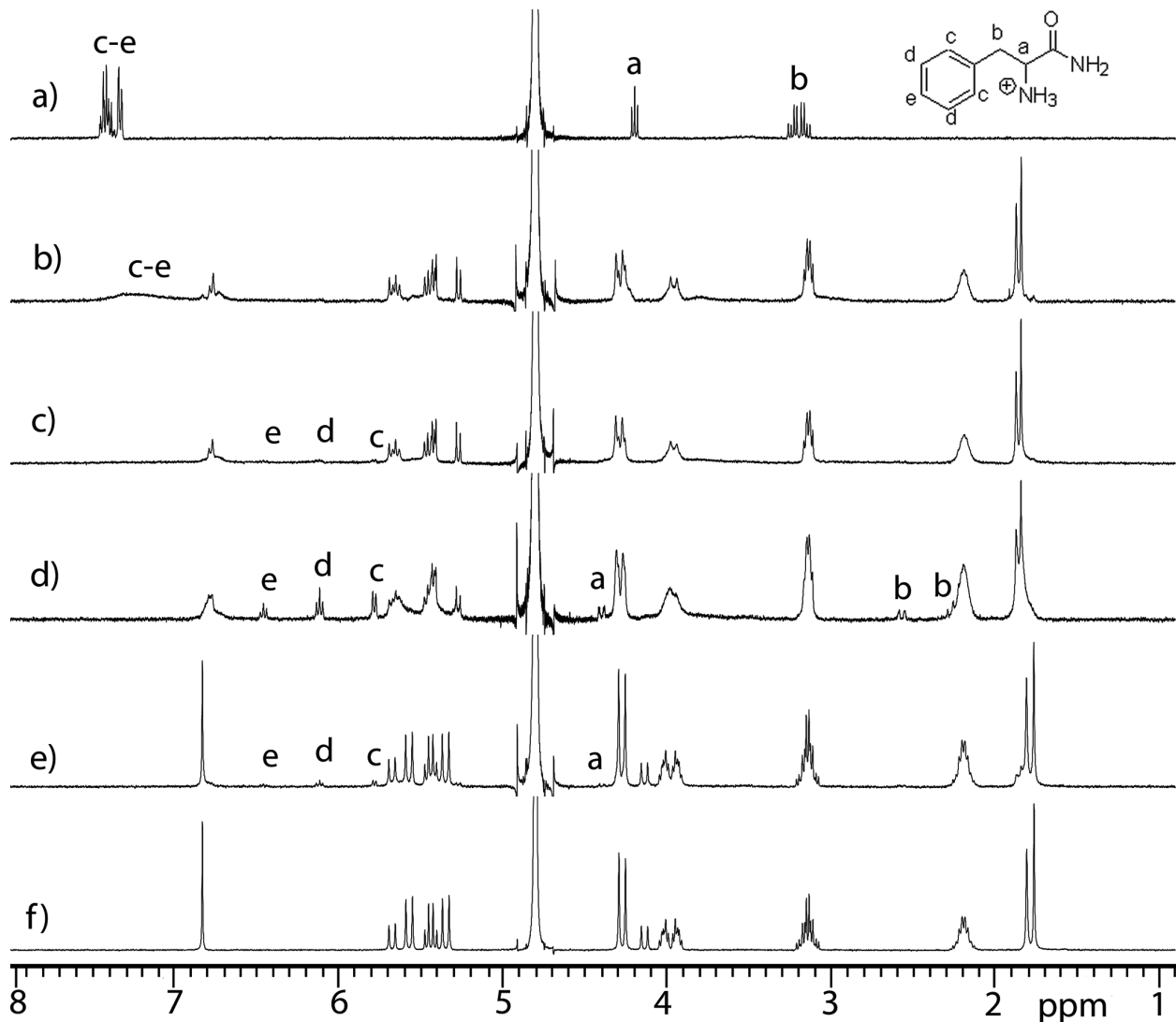


**Figure 3.** <sup>1</sup>H NMR spectra recorded (400 MHz, RT, 20 mM NaH<sub>2</sub>PO<sub>4</sub> buffered D<sub>2</sub>O, pD 7.40) for: a) H-Phe-NH<sub>2</sub> (5 mM), b) **1** (1 mM) and H-Phe-NH<sub>2</sub> (2 mM), c) **1** (1 mM) and H-Phe-NH<sub>2</sub> (1.5 mM), d) **1** (1 mM) and H-Phe-NH<sub>2</sub> (1 mM), e) **1** (1 mM) and H-Phe-NH<sub>2</sub> (0.5 mM), f) **1** (2 mM).

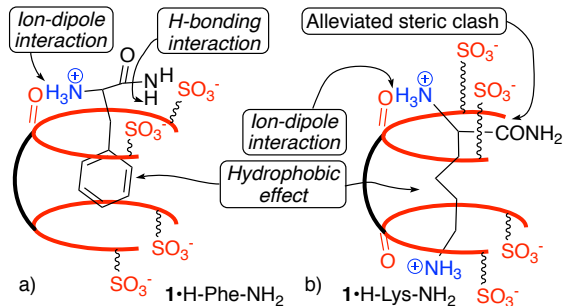


**Figure 4.** Schematic illustrations of the geometry of: a) **1•H-Phe-NH<sub>2</sub>** and b) **1•H-Lys-NH<sub>2</sub>** complexes.

In the <sup>1</sup>H NMR experiments we often observed substantial upfield shifts for guest resonances at 1:1 host:guest stoichiometry which moved back toward the position for complexed guest at 1:2 host:guest ratios which suggested the formation of 1:1 complexes. We constructed Job plots<sup>26</sup> to further establish the 1:1 host:guest stoichiometry in select cases where the resonances were sharp enough to be easily monitored. For example, Figure 5 shows a Job plot constructed for mixtures of **1** and H-Lys-NH<sub>2</sub> at a constant total concentration of 1 mM in phosphate buffered D<sub>2</sub>O (pD 7.40). The chemical shift of H<sub>f</sub> of the host was monitored. As can readily be seen, the Job plot displays a maximum at a mole fraction of 0.5 which firmly establishes the 1:1 absolute stoichiometry of the **1•H-Lys-NH<sub>2</sub>** complex. A related Job plot was constructed to confirm the 1:1 stoichiometry of the **1•H-Arg-NH<sub>2</sub>** complex.

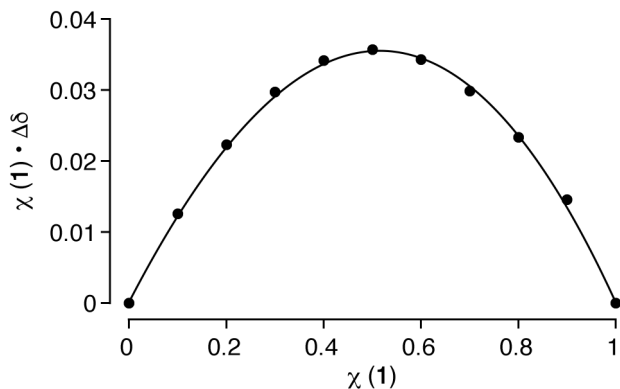


**Figure 5.** Job plot constructed for the interaction of **1** with H-Lys-NH<sub>2</sub> ([**1**] + [H-Lys-NH<sub>2</sub>] = 1 mM) monitoring the chemical shift of H<sub>f</sub> on **1** by <sup>1</sup>H NMR spectroscopy (600 MHz, RT, 20 mM NaH<sub>2</sub>PO<sub>4</sub> buffered D<sub>2</sub>O, pD 7.40). The solid line serves as a guide for the eye.

**Isothermal Titration Calorimetry (ITC) Determination of Host•Guest Energetics.** The substantial broadening and intermediate exchange kinetics observed in the <sup>1</sup>H NMR spectra of the complexes of **1** and **2** with amino acid amide guests complicates the use of NMR to determine binding constants. Accordingly, we turned to ITC to determine the thermodynamic parameters for binding. Figure 6a shows a representative ITC thermogram recorded for the titration of **1** (100 μM) in the ITC cell with a solution of H-Phe-NH<sub>2</sub> (1 mM) in the ITC syringe and the fitting of the data to a 1:1 binding model using the PEAQ ITC analysis software (Figure 6b). In this manner, we were able to extract K<sub>a</sub> = 2.62 × 10<sup>6</sup> M<sup>-1</sup> and ΔH = -17.1 kcal mol<sup>-1</sup> for the **1**•H-Phe-NH<sub>2</sub> complex. Analogous ITC titrations were performed for the complexation between hosts **1** and **2** and the remainder of the amino acid amides, amino acids, and N-acetyl amino acid amides (Supporting Information) and the results are presented in Table 1.

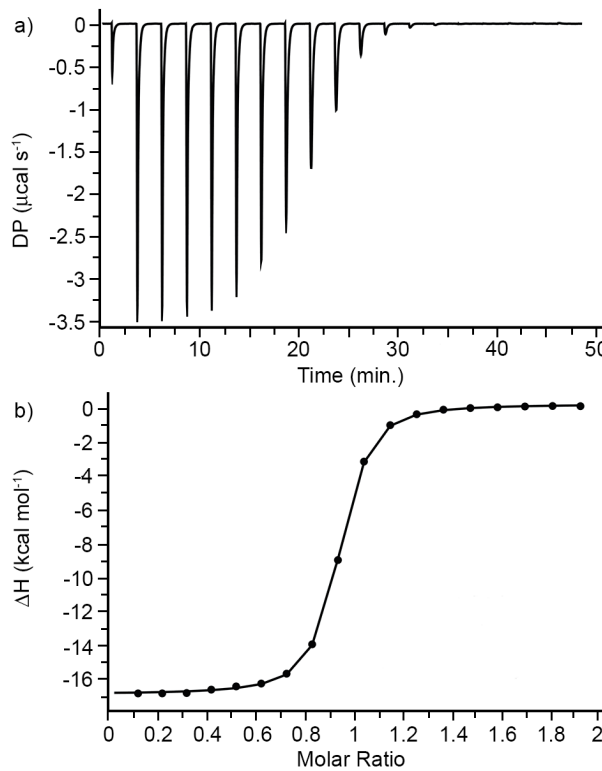


**Figure 6.** a) Thermogram obtained during the titration of **1** (100  $\mu$ M) in the cell with H-Phe-NH<sub>2</sub> (1 mM) in the syringe (298.0 K, 20 mM sodium phosphate buffered H<sub>2</sub>O, pH 7.4) and b) fitting of the data to a 1:1 binding model with  $K_a = 2.62 \times 10^6 \text{ M}^{-1}$  and  $\Delta H = -17.1 \text{ kcal mol}^{-1}$ .

**Table 1.** Thermodynamic parameters obtained by ITC for the interaction of **1** and **2** with the amino acid amides, N-acetyl amino amides, and amino acids. No heat changes were observed with Asp and Glu. (n.b = No heat evolved)

Guest	Host <b>1</b>				Host <b>2</b>			
	$K_a / \text{M}^{-1}$	$\Delta G / \text{kcal mol}^{-1}$	$\Delta H / \text{kcal mol}^{-1}$	$-\Delta S / \text{kcal mol}^{-1}$	$K_a / \text{M}^{-1}$	$\Delta G / \text{kcal mol}^{-1}$	$\Delta H / \text{kcal mol}^{-1}$	$-\Delta S / \text{kcal mol}^{-1}$
Aromatic Sidechain								
H-Phe-NH <sub>2</sub>	$2.62 \times 10^6$	-8.76	$-17.1 \pm 0.04$	8.36	$3.24 \times 10^6$	-8.88	$-17.3 \pm 0.07$	8.45
H-Phe-CO <sub>2</sub> <sup>-</sup>	$7.87 \times 10^4$	-6.68	$-12.5 \pm 0.153$	5.83	$9.61 \times 10^4$	-6.80	$-7.23 \pm 0.074$	0.432
Ac-Phe-NH <sub>2</sub>	$4.17 \times 10^3$	-4.94	$-8.95 \pm 0.448$	4.01	$2.99 \times 10^4$	-6.11	$-10.1 \pm 0.239$	4.04
Cationic Sidechains								
H-Trp-NH <sub>2</sub>	$2.56 \times 10^5$	-7.38	$-14.8 \pm 0.064$	7.43	$3.98 \times 10^6$	-9.00	$-17.7 \pm 0.07$	8.68
H-Trp-COO <sup>-</sup>	$1.06 \times 10^4$	-5.50	$-7.41 \pm 0.132$	1.91	$1.14 \times 10^5$	-6.90	$-6.93 \pm 0.026$	0.026
AcTrp-NH <sub>2</sub>	$8.40 \times 10^2$	-3.99	$-10.4 \pm 0.854$	6.43	$3.56 \times 10^4$	-6.21	$-5.38 \pm 0.30$	-0.828
Aromatic Sidechain								
H-Tyr-NH <sub>2</sub>	$1.01 \times 10^6$	-8.19	$-15.1 \pm 0.03$	6.89	$9.52 \times 10^5$	-8.16	$-15.6 \pm 0.03$	7.40
H-Tyr-COO <sup>-</sup>	$1.01 \times 10^4$	-5.46	$-8.60 \pm 0.226$	3.14	$2.03 \times 10^4$	-5.88	$-8.76 \pm 0.111$	2.88
AcTyr-NH <sub>2</sub>	$1.26 \times 10^3$	-4.23	$-9.36 \pm 0.371$	5.12	$3.06 \times 10^3$	-4.76	$-8.21 \pm 0.079$	3.45
Cationic Sidechains								
H-His-NH <sub>2</sub>	$2.35 \times 10^4$	-5.97	$-9.72 \pm 0.128$	3.75	$2.61 \times 10^4$	-6.03	$-7.18 \pm 0.104$	1.15
Cationic Sidechains								
H-Lys-NH <sub>2</sub>	$7.43 \times 10^5$	-8.01	$-10.9 \pm 0.02$	2.90	$1.41 \times 10^5$	-7.03	$-9.02 \pm 0.12$	1.99

H-Lys-COO <sup>-</sup>	$3.33 \times 10^2$	-3.44	-11.6 $\pm$ 5.02	8.18	497	-3.68	-2.19 $\pm$ 0.036	-1.49
Ac-Lys-NH <sub>2</sub>	$9.80 \times 10^3$	-5.45	-7.13 $\pm$ 0.220	1.68	$8.06 \times 10^3$	-5.33	-2.84 $\pm$ 0.078	-2.49
H-Arg-NH <sub>2</sub>	$7.09 \times 10^5$	-7.98	-11.6 $\pm$ 0.02	3.57	$8.26 \times 10^4$	-6.71	-8.84 $\pm$ 0.058	2.13
H-Arg-COO <sup>-</sup>	$1.51 \times 10^3$	-4.34	-3.93 $\pm$ 0.099	-0.416	$2.39 \times 10^3$	-4.61	-9.82 $\pm$ 0.386	5.21
AcArg-NH <sub>2</sub>	$8.13 \times 10^3$	-5.34	-6.84 $\pm$ 0.178	1.50	$7.87 \times 10^3$	-5.32	-5.44 $\pm$ 0.248	0.119
Non-aromatic polar sidechains								
H-Gln-NH <sub>2</sub>	$1.47 \times 10^4$	-5.69	-5.71 $\pm$ 0.213	0.02	$7.25 \times 10^3$	-5.27	-2.82 $\pm$ 0.69	-2.44
H-Ser-NH <sub>2</sub>	$1.25 \times 10^4$	-5.59	-0.867 $\pm$ 0.007	-4.73	$1.90 \times 10^3$	-4.47	0.944 $\pm$ 0.185	-5.42
H-Thr-NH <sub>2</sub>	$8.33 \times 10^3$	-5.35	-0.546 $\pm$ 0.112	-4.80	n.b	n.b	n.b	n.b
H-Asn-NH <sub>2</sub>	$1.44 \times 10^3$	-4.31	1.42 $\pm$ 1.22	-5.73	$1.35 \times 10^3$	-4.27	-1.62 $\pm$ 0.012	-2.66
H-Met-NH <sub>2</sub>	$1.32 \times 10^5$	-6.99	-13.1 $\pm$ 0.04	6.08	$8.85 \times 10^4$	-6.75	-11.7 $\pm$ 0.04	4.97
Hydrophobic aliphatic sidechains								
H-Ile-NH <sub>2</sub>	$9.43 \times 10^4$	-6.79	-10.8 $\pm$ 0.04	4.02	$1.68 \times 10^5$	-7.13	-9.18 $\pm$ 0.085	2.05
H-Val-NH <sub>2</sub>	$1.40 \times 10^4$	-5.66	-10.1 $\pm$ 0.085	4.40	$2.15 \times 10^4$	-5.91	-4.66 $\pm$ 0.142	-1.26
H-Leu-NH <sub>2</sub>	$2.85 \times 10^5$	-7.44	-9.80 $\pm$ 0.027	2.35	$2.29 \times 10^5$	-7.31	-8.20 $\pm$ 0.43	0.891
H-Pro-NH <sub>2</sub>	$5.75 \times 10^3$	-5.13	-5.43 $\pm$ 0.149	0.299	$1.70 \times 10^4$	-5.77	-5.26 $\pm$ 0.146	-0.510
H-Ala-NH <sub>2</sub>	408	-3.56	-5.32 $\pm$ 0.545	1.76	515	-3.70	-2.77 $\pm$ 0.130	-0.930
H-Gly-NH <sub>2</sub>	80.6	-2.60	-3.88 $\pm$ 0.742	1.28	115	-2.81	-1.36 $\pm$ 0.125	-1.46

*Discussion of Trends in the Thermodynamic Parameters.* The dynamic range of binding constants presented in Table 1 spans the range from  $10^2$  M<sup>-1</sup> to above  $10^6$  M<sup>-1</sup>. Given the constraints of this relatively narrow range, we have been able to discern some trends in the thermodynamic parameters and present them here grouped according to the chemical nature of the amino acid amide side chain (e.g. anionic, cationic, aromatic, hydrophobic aliphatic, polar). Firstly, in agreement with our <sup>1</sup>H NMR measurements, no heat is evolved during the titration of **1** or **2** with the H-Asp-NH<sub>2</sub> and H-Glu-NH<sub>2</sub> and we therefore conclude that no binding occurs with these amino acid amides that contain anionic side chains. This result is in accord with the well-known preference of the CB[n] cavity for hydrophobic and neutral binding epitopes over hydrophilic and anionic groups.<sup>3,4e</sup> Second, we find that the aromatic amino acid amides (H-Phe-NH<sub>2</sub>, H-Trp-NH<sub>2</sub>, H-Tyr-NH<sub>2</sub>) form the tightest complexes with **1** and **2** with K<sub>a</sub> values that exceed  $10^6$  M<sup>-1</sup> and with large enthalpic driving forces in the range of -15 – -18 kcal mol<sup>-1</sup>. This trend is not so surprising in light of the hydrophobicity of the aromatic rings of the amino acid amides, the ability of aromatic walls of **1** and **2** to engage in  $\pi$ – $\pi$  interactions with the guest, and of course the precedent from the work of Kim, Inoue, Nau and Urbach that showed that peptides with aromatic sidechains at the N-terminus are bound selectively by CB[7].<sup>11b,16b,24,27</sup>

Macrocyclic CB[7] has been reported to bind Phe-Gly-Gly ( $K_a = 2.8 \times 10^6 \text{ M}^{-1}$ ), Phe-Gly ( $K_a = 3 \times 10^7 \text{ M}^{-1}$ ), Tyr-Gly ( $K_a = 3.6 \times 10^6 \text{ M}^{-1}$ ), and Trp-Gly ( $K_a = 5.6 \times 10^5 \text{ M}^{-1}$ ) with affinities that are comparable to those observed for **1** and **2**.<sup>11b,27</sup> For H-Phe-NH<sub>2</sub> and H-Trp-NH<sub>2</sub>, the larger host **2** binds stronger than **1** as expected based on its larger cavity size.<sup>18a,20a</sup> H-His-NH<sub>2</sub> with its hydrophilic and charged aromatic sidechain is bound significantly weaker to both **1** and **2** ( $K_a \approx 10^4 \text{ M}^{-1}$ ) and with significantly lower enthalpic driving force. Third, H-Lys-NH<sub>2</sub> and H-Arg-NH<sub>2</sub> which are dicationic at neutral pH and contain 4-5 C-atoms between cationic N-atoms bind toward **1** with affinities ( $K_a \approx 7 \times 10^5 \text{ M}^{-1}$ ) that are only slightly lower than the aromatic amino acid amides. They do not reach the very high affinity typically observed for diammonium ion complexes with cucurbiturils presumably because of the presence of the CONH<sub>2</sub> group. Host **1** displays higher affinity than **2** toward H-Lys-NH<sub>2</sub> (5.3-fold) and H-Arg-NH<sub>2</sub> (8.6-fold) because the cavity of **1** is smaller than **2** and prefers narrower (e.g. alkylene) guests as observed previously.<sup>2c</sup> Fourth, among the amino acid amides with polar side chains we find that H-Met-NH<sub>2</sub> binds most strongly to **1** ( $K_a = 1.32 \times 10^5 \text{ M}^{-1}$ ) and **2** ( $K_a = 8.85 \times 10^4 \text{ M}^{-1}$ ) with substantial enthalpic driving forces. This is not surprising given that methionine has both the largest sidechain surface area and the least favourable free energy of transfer from cyclohexane to water which enhances the hydrophobic driving force for complexation.<sup>11b</sup> The remaining polar amino acid amides (H-Gln-NH<sub>2</sub>, H-Asn-NH<sub>2</sub>, H-Thr-NH<sub>2</sub>, H-Ser-NH<sub>2</sub>) bind more weakly with  $K_a$  in the  $10^2 - 10^4 \text{ M}^{-1}$  range which reflects the need to desolvate the side chains polar OH and CONH<sub>2</sub> functional groups as they enter the host cavity. As expected, a comparison of the binding constant of **1** toward H-Gln-NH<sub>2</sub> versus H-Asn-NH<sub>2</sub> and H-Thr-NH<sub>2</sub> versus H-Ser-NH<sub>2</sub> reveals that the compound with the additional CH<sub>2</sub>-group in the sidechain is the stronger binder.<sup>3</sup> Finally, the amino acid amides with hydrophobic aliphatic sidechains (H-Ile-NH<sub>2</sub>, H-Val-NH<sub>2</sub>,

H-Leu-NH<sub>2</sub>, H-Pro-NH<sub>2</sub>) bind to **1** and **2** with  $K_a$  values in the  $6 \times 10^3$  to  $3 \times 10^5$  M<sup>-1</sup> range and  $\Delta H$  values in the -5 to -7.5 kcal mol<sup>-1</sup> range with; host **2** is generally the tighter binder. The order of binding affinity toward **1** and **2** follows the order H-Pro-NH<sub>2</sub> < H-Val-NH<sub>2</sub> < H-Ile-NH<sub>2</sub> < H-Leu-NH<sub>2</sub>. As expected, H-Pro-NH<sub>2</sub> and H-Val-NH<sub>2</sub> which have fewer C-atoms in the sidechain relative to H-Ile-NH<sub>2</sub> and H-Leu-NH<sub>2</sub> (e.g. 3 versus 4) bind more weakly. We speculate that the pyrrolidine ring of H-Pro-NH<sub>2</sub> displays reduced affinity because the preferences of ion-dipole and hydrophobic effect cannot be fully satisfied simultaneously. Finally, H-Gly-NH<sub>2</sub> and H-Ala-NH<sub>2</sub> with no or minimal side chains exhibit low binding affinity toward **1** and **2** ( $K_a \leq 10^3$  M<sup>-1</sup>) probably due to weak electrostatic effects.

*Influence of N-acetylation and C-amidation.* We measured the binding of **1** and **2** toward the unmodified amino acid and N-acetyl amino acid forms of phenylalanine, tryptophan, tyrosine, lysine, and arginine (Table 1). We hypothesized that the amino acid amides would bind more strongly than the amino acids themselves due to the absence of unfavorable CO<sub>2</sub><sup>-</sup> to SO<sub>3</sub><sup>-</sup> and/or C=O portal interactions. Similarly, we expected that the amino acid amides would bind more strongly than the N-acetyl amino acid amides due to the loss of NH<sub>3</sub><sup>+</sup> to O=C ion dipole in the later. These interactions are presented schematically in Figure 7. For **1**•H-Phe-NH<sub>2</sub> (**2**•H-Phe-NH<sub>2</sub>) the loss of NH<sub>3</sub><sup>+</sup>••O=C ion dipole interactions costs 3.8 kcal mol<sup>-1</sup> (2.8 kcal mol<sup>-1</sup>) whereas the introduction of unfavourable CO<sub>2</sub><sup>-</sup> electrostatic interactions costs 2.1 kcal mol<sup>-1</sup> (2.1 kcal mol<sup>-1</sup>). Related losses of free energy were observed for the complexes of **1** (**2**) toward H-Trp-NH<sub>2</sub> (**1**: 3.4 and 1.9 kcal mol<sup>-1</sup>; **2**: 2.8 and 2.1 kcal mol<sup>-1</sup>) and H-Tyr-NH<sub>2</sub> (**1**: 3.96 and 2.7 kcal mol<sup>-1</sup>; **2**: 3.4 and 2.3 kcal mol<sup>-1</sup>) upon acylation of the N-terminus and introduction of a C-terminal CO<sub>2</sub><sup>-</sup> group. In contrast, for the dicationic amino acids H-Lys-NH<sub>2</sub> (**1**: 2.6 and 4.6 kcal

mol<sup>-1</sup>; **2**: 1.7 and 3.4 kcal mol<sup>-1</sup>) and H-Arg-NH<sub>2</sub> (**1**: 2.6 and 3.6 kcal mol<sup>-1</sup>; **2**: 1.4 and 2.1 kcal mol<sup>-1</sup>) the introduction of the CO<sub>2</sub><sup>-</sup> group is energetically more costly than removal of the NH<sub>3</sub><sup>+</sup>•••O=C ion dipole interactions. We rationalize this observation based on the fact that for Lys and Arg the diammonium spans the two C=O portals which conformationally fixes the CO<sub>2</sub><sup>-</sup> group within the cavity near the electrostatically negative C=O portals of **1** or **2**. Accordingly, we conclude that ion-dipole interactions play a primary role in determining the strength of complexes between tetraanionic **1** (**2**) and amino acid amides but that secondary electrostatic interactions can significantly modulate binding affinity.

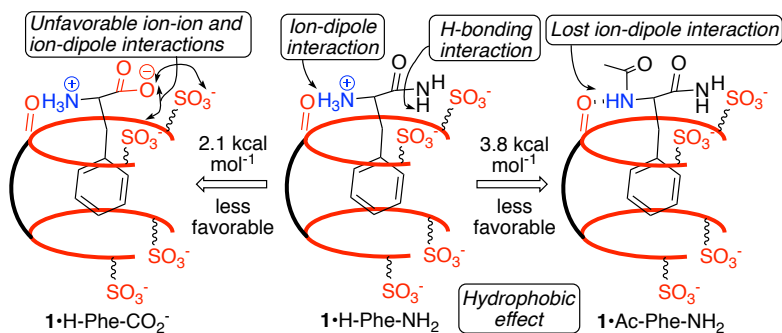


**Figure 7.** Schematic illustration of the complexes of **1** with H-Phe-CO<sub>2</sub><sup>-</sup>, H-Phe-NH<sub>2</sub>, and Ac-Phe-NH<sub>2</sub> along with their driving forces and relative stabilities.

*Influence of Neighboring Residues.* We were inspired by the recent work of Urbach which showed that CB[8] is capable of simultaneously binding two adjacent sidechains within the context of a tripeptide with nanomolar affinity.<sup>28</sup> Accordingly, we sought to determine if acyclic cucurbiturils like **1** or **2** could recognize an N-terminal Phe along with an adjacent residues sidechain. We selected FGA as control tripeptide along with six tripeptides (FFA, FLA, FVA, FIA, FPA, FKA) with adjacent aromatic, hydrophobic, or cationic sidechain. ITC experiments were performed for these tripeptides toward **1** and **2** and the results are given in Table 2. First,

we found that the **1**•FGA complex ( $K_a = 1.48 \times 10^6 \text{ M}^{-1}$ ;  $\Delta H = -8.42 \text{ kcal mol}^{-1}$ ) is of comparable affinity and enthalpic driving force to the **1**•H-Phe-NH<sub>2</sub> complex ( $K_a = 2.62 \times 10^6 \text{ M}^{-1}$ ;  $\Delta H = -8.76 \text{ kcal mol}^{-1}$ ). Interestingly, compared to the **1**•FGA complex all of the tripeptides with aromatic, hydrophobic, or cationic adjacent residues bind 6 to 22-fold more weakly. The **1**•FPA complex is the weakest with  $K_a = 6.62 \times 10^4 \text{ M}^{-1}$  presumably due to the loss of a potential N-H••O=C H-bond due to the tertiary amide bond at proline. All these results suggest that the cavity of **1** cannot expand to accommodate a second residue and that the second residue experiences unfavourable steric interactions which reduces affinity. The binding to **1** to FVA was of particular relevance to our planned binding experiments toward insulin since the N-terminus of insulin also has the FV sequence. Unfortunately, the **1**•FVA complex has similar affinity to all the other tripeptides tested. The behaviour of **2** is more subtle and the affinity toward all the tripeptides cluster around  $10^5 \text{ M}^{-1}$ . Despite the previously demonstrated ability of **1** and **2** to expand its cavity to accommodate larger guests with roughly circular cross sections in the form of adamantanes, steroids, and even carbon nanotubes,<sup>20a,29</sup> they prefer to bind a single narrower alkyl and phenyl ring when given the option.<sup>18a,18c,30</sup>

**Table 2.** Thermodynamic parameters obtained by ITC for the interaction of **1** and **2** with tripeptides

Guest	Host <b>1</b>				Host <b>2</b>			
	$K_a / \text{M}^{-1}$	$\Delta G / \text{kcal mol}^{-1}$	$\Delta H / \text{kcal mol}^{-1}$	$-\Delta S / \text{kcal mol}^{-1}$	$K_a / \text{M}^{-1}$	$\Delta G / \text{kcal mol}^{-1}$	$\Delta H / \text{kcal mol}^{-1}$	$-\Delta S / \text{kcal mol}^{-1}$
FGA	$1.48 \times 10^6$	-8.42	$-13.3 \pm 0.038$	4.93	$1.20 \times 10^5$	-6.93	$-18.1 \pm 0.697$	11.1
FFA	$2.52 \times 10^5$	-7.37	$-13.7 \pm 0.097$	6.37	$1.22 \times 10^5$	-6.94	$-12.5 \pm 0.27$	5.56
FLA	$1.57 \times 10^5$	-7.09	$-13.4 \pm 0.201$	6.27	$2.59 \times 10^5$	-7.39	$-10.1 \pm 0.176$	2.72
FIA	$1.40 \times 10^5$	-7.02	$-13.3 \pm 0.121$	6.32	$2.62 \times 10^5$	-7.39	$-10.0 \pm 0.131$	2.62
FVA	$3.89 \times 10^5$	-7.63	$-12.7 \pm 0.076$	5.07	$3.84 \times 10^5$	-7.62	$-11.7 \pm 0.03$	4.13
FPA	$6.62 \times 10^4$	-6.58	$-12.4 \pm 0.169$	5.81	$1.06 \times 10^5$	-6.86	$-8.16 \pm 0.207$	1.30
FKA	$2.34 \times 10^5$	-7.32	$-14.4 \pm 0.224$	7.03	$5.32 \times 10^4$	-6.45	$-9.29 \pm 0.814$	2.84

*Molecular Recognition of Insulin by **1**, **2**, and CB[7].* Finally, we decided to study the interaction of **1** and **2** with a protein. As the model protein we selected insulin based on the pioneering work of the Urbach group.<sup>16a</sup> Accordingly, we sought to measure the binding affinity of **1** and **2** toward insulin and compare the results to those measured previously with CB[7]. ITC binding studies were performed in our standard 20 mM sodium phosphate buffered water at pH 7.4 containing 4 mM EDTA which sequesters metal ions that promote oligomerization of insulin. Table 3 shows the results of the ITC studies which indicates that CB[7] binds insulin the strongest followed closely by **2** and then **1**. The affinity of the insulin•CB[7] complex ( $5.59 \times 10^5 \text{ M}^{-1}$ ) is slightly lower than that measured previously by Urbach ( $K_a = 1.5 \times 10^6 \text{ M}^{-1}$ ) which we attribute to the less competitive 10 mM sodium phosphate buffer they used.<sup>16a</sup> Satisfyingly, the binding constants measured for **1** and **2** toward insulin are comparable to those measured toward the FVA peptide which indicates that secondary electrostatic interactions between the tetraanionic hosts and insulin are not energetically costly. In comparison the  $K_a$  values measured for the interaction of H-Phe-NH<sub>2</sub> with **1** and **2** are about 10-fold higher (Table 1) which confirms the sensitivity of **1** and **2** to the steric bulk at the neighboring amino acid residue.

**Table 3.** Thermodynamic parameters obtained by ITC for the interaction of CB [7], **1**, and **2** with Insulin.

HOST	$K_a / \text{M}^{-1}$	$\Delta G$	$\Delta H$	$-\Delta S$
CB[7]	$5.59 \times 10^5$	-7.84	$-8.97 \pm 0.232$	1.13
<b>1</b>	$1.32 \times 10^5$	-6.99	$-16.9 \pm 0.225$	9.91
<b>2</b>	$3.47 \times 10^5$	-7.56	$-10.4 \pm 0.151$	2.86

**Conclusions.** In summary, we have delineated the binding properties of acyclic CB[n]-type receptors **1** and **2** toward 19 amino acid amides by a combination of <sup>1</sup>H NMR spectroscopy and ITC. The sidechains typically undergo cavity inclusion whereas the N-terminus binds at the

C=O portal by ion-dipole and ion-SO<sub>3</sub><sup>-</sup> interactions. Binding constants range from <10<sup>2</sup> (for anionic and small sidechains) to  $\approx 10^6$  M<sup>-1</sup> for amino acid amides with aromatic (Phe, Trp, Tyr) and even cationic (Lys and Arg) sidechains. The broader range of residues undergoing high affinity binding by **1** and **2** stands in contrast to that of CB[7] which suggests a broad range of potential applications. Studies of the binding of **1** and **2** toward the N-acetyl amino acid amides and the free amino acids allowed us to quantify the energetic contributions of electrostatics to the binding process. For example, the removal of the NH<sub>3</sub><sup>+</sup>•••O=C ion-dipole interactions (e.g. **1**•H-Phe-NH<sub>2</sub> versus **1**•Ac-Phe-NH<sub>2</sub>) costs 3.8 kcal mol<sup>-1</sup> whereas the introduction of unfavorable CO<sub>2</sub><sup>-</sup> electrostatic interactions costs 2.1 kcal mol<sup>-1</sup>. Given the propensity of acyclic CB[n] to expand their cavity to bind to large guests, we explored the possibility of **1** or **2** simultaneously binding two amino acid sidechains but observed no evidence for such phenomena. Finally, we demonstrate that **1** and **2** bind to insulin with affinities similar to CB[7]. Overall, the work demonstrates that acyclic CB[n] have a broad affinity toward aromatic and cationic sidechains of N-terminal amino acids which suggests that acyclic CB[n] have a bright future as a component of enzyme assays, sensor arrays, and biotechnology applications.

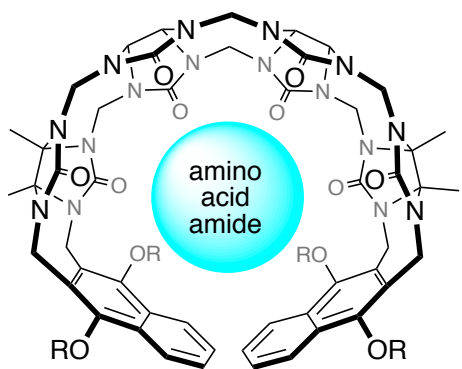
**Experimental Details.** Compounds **1** and **2** were prepared according to the literature procedures.<sup>31</sup> The amino acids, amino amides, and N-acetyl amino amides were purchased from Bachem, Chem-Impex, Alfa Aesar, and Acros Organics and used without further purification. <sup>1</sup>H and <sup>13</sup>C NMR spectra were measured on 400 MHz and 500 MHz spectrometers (100 MHz and 125 MHz for <sup>13</sup>C NMR, respectively) at room temperature in 20 mM NaH<sub>2</sub>PO<sub>4</sub> buffered D<sub>2</sub>O at pD 7.4. Isothermal titration calorimetry was performed using a PEAQ-ITC (Malvern) instrument and the data was analyzed using the software provided by the manufacturer. The ITC

experiments were performed in 20 mM sodium phosphate buffered H<sub>2</sub>O (pH 7.4) at 298.15 K and generally consisted of a series of 19 injections (2  $\mu$ L each) with a stirring speed of 750 rpm.

**Disclosure Statement.** L.I. is an inventor on patents related to the use of **1** and **2** in biomedical applications.

**Funding.** We thank the National Science Foundation (CHE-1404911 and CHE-1807486 to L. I.) and the University of Maryland (LSAMP and McNair Fellowships to S. Z.) for financial support.

**Table of Contents Graphic:**



Calabadion 2-amino acid

R = (CH<sub>2</sub>)<sub>3</sub>SO<sub>3</sub>Na

K<sub>d</sub> as low as 250 nM

## References.

- 1) a) Kim, J.; Jung, I.-S.; Kim, S.-Y.; Lee, E.; Kang, J.-K.; Sakamoto, S.; Yamaguchi, K.; Kim, K., *J. Am. Chem. Soc.* **2000**, *122*, 540-541; b) Day, A. I.; Arnold, A. P.; Blanch, R. J.; Snushall, B., *J. Org. Chem.* **2001**, *66*, 8094-8100.
- 2) a) Assaf, K. I.; Nau, W. M., *Chem. Soc. Rev.* **2015**, *44*, 394-418; b) Isaacs, L., *Acc. Chem. Res.* **2014**, *47*, 2052-2062; c) Ganapati, S.; Isaacs, L., *Isr. J. Chem.* **2018**, *58*, 250-263; d) Lee, J. W.; Samal, S.; Selvapalam, N.; Kim, H.-J.; Kim, K., *Acc. Chem. Res.* **2003**, *36*, 621-630; e) Lizal, T.; Sindelar, V., *Isr. J. Chem.* **2018**, *58*, 326-333; f) Cong, H.; Ni, X. L.; Xiao, X.; Huang, Y.; Zhu, Q.-J.; Xue, S.-F.; Tao, Z.; Lindoy, L. F.; Wei, G., *Org. Biomol. Chem.* **2016**, *14*, 4335-4364.
- 3) Mock, W. L.; Shih, N.-Y., *J. Org. Chem.* **1986**, *51*, 4440-4446.
- 4) a) Biedermann, F.; Uzunova, V. D.; Scherman, O. A.; Nau, W. M.; De Simone, A., *J. Am. Chem. Soc.* **2012**, *134*, 15318-15323; b) Liu, S.; Ruspic, C.; Mukhopadhyay, P.; Chakrabarti, S.; Zavalij, P. Y.; Isaacs, L., *J. Am. Chem. Soc.* **2005**, *127*, 15959-15967; c) Rekharsky, M. V.; Mori, T.; Yang, C.; Ko, Y. H.; Selvapalam, N.; Kim, H.; Sobransingh, D.; Kaifer, A. E.; Liu, S.; Isaacs, L.; Chen, W.; Moghaddam, S.; Gilson, M. K.; Kim, K.; Inoue, Y., *Proc. Natl. Acad. Sci. U. S. A.* **2007**, *104*, 20737-20742; d) Cao, L.; Sekutor, M.; Zavalij, P. Y.; Mlinaric-Majerski, K.; Glaser, R.; Isaacs, L., *Angew. Chem. Int. Ed.* **2014**, *53*, 988-993; e) Jeon, W. S.; Moon, K.; Park, S. H.; Chun, H.; Ko, Y. H.; Lee, J. Y.; Lee, E. S.; Samal, S.; Selvapalam, N.; Rekharsky, M. V.; Sindelar, V.; Sobransingh, D.; Inoue, Y.; Kaifer, A. E.; Kim, K., *J. Am. Chem. Soc.* **2005**, *127*, 12984-12989; f) Moghaddam, S.; Yang, C.; Rekharsky, M.; Ko, Y. H.; Kim, K.; Inoue, Y.; Gilson, M. K., *J. Am. Chem. Soc.* **2011**, *133*, 3570-3581.
- 5) a) Barrow, S. J.; Kasera, S.; Rowland, M. J.; del Barrio, J.; Scherman, O. A., *Chem. Rev.* **2015**, *115*, 12320-12406; b) del Barrio, J.; Ryan, S. T. J.; Jambrina, P. G.; Rosta, E.; Scherman, O. A., *J. Am. Chem. Soc.* **2016**, *138*, 5745-5748; c) Ko, Y. H.; Kim, E.; Hwang, I.; Kim, K., *Chem. Commun.* **2007**, 1305-1315.
- 6) a) Palma, A.; Artelsmair, M.; Wu, G.; Lu, X.; Barrow, S. J.; Uddin, N.; Rosta, E.; Masson, E.; Scherman, O. A., *Angew. Chem., Int. Ed.* **2017**, *56*, 15688-15692; b) Masson, E.; Raeisi, M.; Kotturi, K., *Isr. J. Chem.* **2018**, *58*, 413-434; c) Wang, R.; Yuan, L.; Macartney, D. H., *J. Org. Chem.* **2006**, *71*, 1237-1239.
- 7) a) Cao, L.; Hettiarachchi, G.; Briken, V.; Isaacs, L., *Angew. Chem. Int. Ed.* **2013**, *52*, 12033-12037; b) Chen, H.; Chan, J. Y. W.; Li, S.; Liu, J. J.; Wyman, I. W.; Lee, S. M. Y.; Macartney, D. H.; Wang, R., *RSC Adv.* **2015**, *5*, 63745-63752; c) Yin, H.; Wang, R., *Isr. J. Chem.* **2017**, *58*, 188-198; d) Wheate, N. J.; Limantoro, C., *Supramol. Chem.* **2016**, *28*, 849-856; e) Ghosh, I.; Nau, W. M., *Adv. Drug Delivery Rev.* **2012**, *64*, 764-783; f) Saleh, N. I.; Ghosh, I.; Nau, W. M., *Monogr. Supramol. Chem.* **2013**, *13*, 164-212; g) Dong, N.; Xue, S.-F.; Zhu, Q.-J.; Tao, Z.; Zhao, Y.; Yang, L.-X., *Supramol. Chem.* **2008**, *20*, 659-665; h) Jeon, Y. J.; Kim, S.-Y.; Ko, Y. H.; Sakamoto, S.; Yamaguchi, K.; Kim, K., *Org. Biomol. Chem.* **2005**, *3*, 2122-2125.
- 8) a) Ghale, G.; Nau, W. M., *Acc. Chem. Res.* **2014**, *47*, 2150-2159; b) Shcherbakova, E. G.; Zhang, B.; Gozem, S.; Minami, T.; Zavalij Peter, Y.; Pushina, M.; Isaacs, L.; Anzenbacher, P. J., *J. Am. Chem. Soc.* **2017**, *139*, 14954-14960.
- 9) Jang, Y.; Jang, M.; Kim, H.; Lee, S. J.; Jin, E.; Koo, J. Y.; Hwang, I.-C.; Kim, Y.; Ko, Y. H.; Hwang, I.; Oh, J. H.; Kim, K., *Chem* **2017**, *3*, 641-651.

10) a) Yang, H.; Yuan, B.; Zhang, X.; Scherman, O. A., *Acc. Chem. Res.* **2014**, *47*, 2106-2115; b) Appel, E. A.; del Barrio, J.; Loh, X. J.; Scherman, O. A., *Chem. Soc. Rev.* **2012**, *41*, 6195-6214; c) Liu, J.; Lan, Y.; Yu, Z.; Tan, C. S. Y.; Parker, R. M.; Abell, C.; Scherman, O. A., *Acc. Chem. Res.* **2017**, *50*, 208-217; d) Tian, J.; Zhou, T.-Y.; Zhang, S.-C.; Aloni, S.; Altoe, M. V.; Xie, S.-H.; Wang, H.; Zhang, D.-W.; Zhao, X.; Liu, Y.; Li, Z.-T., *Nat. Commun.* **2014**, *5*, 5574; e) Tian, J.; Chen, L.; Zhang, D.-W.; Liu, Y.; Li, Z.-T., *Chem. Commun.* **2016**, *52*, 6351-6362; f) Ahn, Y.; Jang, Y.; Selvapalam, N.; Yun, G.; Kim, K., *Angew. Chem. Int. Ed.* **2013**, *52*, 3140-3144.

11) a) Heitmann, L. M.; Taylor, A. B.; Hart, P. J.; Urbach, A. R., *J. Am. Chem. Soc.* **2006**, *128*, 12574-12581; b) Urbach, A. R.; Ramalingam, V., *Isr. J. Chem.* **2011**, *51*, 664-678.

12) a) van Dun, S.; Ottmann, C.; Milroy, L.-G.; Brunsved, L., *J. Am. Chem. Soc.* **2017**, *139*, 13960-13968; b) Hou, C.; Li, J.; Zhao, L.; Zhang, W.; Luo, Q.; Dong, Z.; Xu, J.; Liu, J., *Angew. Chem., Int. Ed.* **2013**, *52*, 5590-5593.

13) Bosmans, R. P. G.; Briels, J. M.; Milroy, L.-G.; de Greef, T. F. A.; Merkx, M.; Brunsved, L., *Angew. Chem., Int. Ed.* **2016**, *55*, 8899-8903.

14) Dang, D. T.; Nguyen, H. D.; Merkx, M.; Brunsved, L., *Angew. Chem., Int. Ed.* **2013**, *52*, 2915-2919.

15) a) Sonzini, S.; Ryan, S. T. J.; Scherman, O. A., *Chem. Commun.* **2013**, *49*, 8779-8781; b) Rowland, M. J.; Atgie, M.; Hoogland, D.; Scherman, O. A., *Biomacromolecules* **2015**, *16*, 2436-2443.

16) a) Chinai, J. M.; Taylor, A. B.; Ryno, L. M.; Hargreaves, N. D.; Morris, C. A.; Hart, P. J.; Urbach, A. R., *J. Am. Chem. Soc.* **2011**, *133*, 8810-8813; b) Ghale, G.; Ramalingam, V.; Urbach, A. R.; Nau, W. M., *J. Am. Chem. Soc.* **2011**, *133*, 7528-7535; c) Logsdon, L. A.; Schardon, C. L.; Ramalingam, V.; Kwee, S. K.; Urbach, A. R., *J. Am. Chem. Soc.* **2011**, *133*, 17087-17092; d) Logsdon, L. A.; Urbach, A. R., *J. Am. Chem. Soc.* **2013**, *135*, 11414-11416; e) Lee, J. W.; Shin, M. H.; Mobley, W.; Urbach, A. R.; Kim, H. I., *J. Am. Chem. Soc.* **2015**, *137*, 15322-15329; f) Li, W.; Bockus, A. T.; Vinciguerra, B.; Isaacs, L.; Urbach, A. R., *Chem. Commun.* **2016**, *52*, 8537-8540.

17) Webber, M. J.; Appel, E. A.; Vinciguerra, B.; Cortinas, A. B.; Thapa, L. S.; Jhunjhunwala, S.; Isaacs, L.; Langer, R.; Anderson, D. G., *Proc. Natl. Acad. Sci. U. S. A.* **2016**, *113*, 14189-14194.

18) a) Zhang, B.; Isaacs, L., *J. Med. Chem.* **2014**, *57*, 9554-9563; b) Zhang, B.; Zavalij, P. Y.; Isaacs, L., *Org. Biomol. Chem.* **2014**, *12*, 2413-2422; c) Gilberg, L.; Zhang, B.; Zavalij, P. Y.; Sindelar, V.; Isaacs, L., *Org. Biomol. Chem.* **2015**, *13*, 4041-4050; d) Zhang, M.; Sigwalt, D.; Isaacs, L., *Chem. Commun.* **2015**, *51*, 14620-14623; e) Sigwalt, D.; Moncelet, D.; Falcinelli, S.; Mandadapu, V.; Zavalij, P. Y.; Day, A.; Briken, V.; Isaacs, L., *ChemMedChem* **2016**, *11*, 980-989.

19) Hettiarachchi, G.; Samanta, S. K.; Falcinelli, S.; Zhang, B.; Moncelet, D.; Isaacs, L.; Briken, V., *Mol. Pharmaceutics* **2016**, *13*, 809-818.

20) a) Ma, D.; Zhang, B.; Hoffmann, U.; Sundrup, M. G.; Eikermann, M.; Isaacs, L., *Angew. Chem. Int. Ed.* **2012**, *51*, 11358-11362; b) Haerter, F.; Simons, J. C. P.; Foerster, U.; Moreno Duarte, I.; Diaz-Gil, D.; Ganapati, S.; Eikermann-Haerter, K.; Ayata, C.; Zhang, B.; Blobner, M.; Isaacs, L.; Eikermann, M., *Anesthesiology* **2015**, *123*, 1337-1349; c) Hoffmann, U.; Grosse-Sundrup, M.; Eikermann-Haerter, K.; Zaremba, S.; Ayata, C.; Zhang, B.; Ma, D.; Isaacs, L.; Eikermann, M., *Anesthesiology* **2013**, *119*, 317-325.

21) Ganapati, S.; Grabitz, S. D.; Murkli, S.; Scheffenbichler, F.; Rudolph, M. I.; Zavalij, P. Y.; Eikermann, M.; Isaacs, L., *Chembiochem* **2017**, *18*, 1583-1588.

22) a) Chen, J.; Liu, Y.; Mao, D.; Ma, D., *Chem. Commun.* **2017**, *53*, 8739-8742; b) Mao, D.; Liang, Y.; Liu, Y.; Zhou, X.; Ma, J.; Jiang, B.; Liu, J.; Ma, D., *Angew. Chem. Int. Ed.* **2017**, *41*, 12614-12618; c) Jiang, S.; Lan, S.; Mao, D.; Yang, X.; Shi, K.; Ma, D., *Chem. Commun.* **2018**, *54*, 9486-9489; d) Mao, W.; Mao, D.; Yang, F.; Ma, D., *Chem. - Eur. J.* **2019**, *25*, 2272-2280.

23) a) Minami, T.; Esipenko, N. A.; Zhang, B.; Isaacs, L.; Nishiyabu, R.; Kubo, Y.; Anzenbacher, P., *J. Am. Chem. Soc.* **2012**, *134*, 20021-20024; b) Minami, T.; Esipenko, N. A.; Akdeniz, A.; Zhang, B.; Isaacs, L.; Anzenbacher, P., *J. Am. Chem. Soc.* **2013**, *135*, 15238-15243; c) Minami, T.; Esipenko, N. A.; Zhang, B.; Isaacs, L.; Anzenbacher, P., *Chem. Commun.* **2014**, *50*, 61-63.

24) Rekharsky, M. V.; Yamamura, H.; Ko, Y. H.; Selvapalam, N.; Kim, K.; Inoue, Y., *Chem. Commun.* **2008**, 2236-2238.

25) Klaerner, F.-G.; Schrader, T., *Acc. Chem. Res.* **2013**, *46*, 967-978.

26) Job, P., *Ann. Chim.* **1928**, *9*, 113-204.

27) Rekharsky, M. V.; Yamamura, H.; Inoue, C.; Kawai, M.; Osaka, I.; Arakawa, R.; Shiba, K.; Sato, A.; Ko, Y. H.; Selvapalam, N.; Kim, K.; Inoue, Y., *J. Am. Chem. Soc.* **2006**, *128*, 14871-14880.

28) a) Hirani, Z.; Taylor, H. F.; Babcock, E. F.; Bockus, A. T.; Varnado, C. D.; Bielawski, C. W.; Urbach, A. R., *J. Am. Chem. Soc.* **2018**, *140*, 12263-12269; b) Smith, L. C.; Leach, D. G.; Blaylock, B. E.; Ali, O. A.; Urbach, A. R., *J. Am. Chem. Soc.* **2015**, *137*, 3663-3669.

29) a) Shen, C.; Ma, D.; Meany, B.; Isaacs, L.; Wang, Y., *J. Am. Chem. Soc.* **2012**, *134*, 7254-7257; b) Lu, X.; Isaacs, L., *Angew. Chem. Int. Ed.* **2016**, *55*, 8076-8080.

30) Lu, X. Y.; Isaacs, L., *Angew. Chem. Int. Ed.* **2016**, *55*, 8076-8080.

31) Ma, D.; Hettiarachchi, G.; Nguyen, D.; Zhang, B.; Wittenberg, J. B.; Zavalij, P. Y.; Briken, V.; Isaacs, L., *Nat. Chem.* **2012**, *4*, 503-510.